Original Research Article

Groundwater depth prediction based on wavelet decomposition-LSTM network

Abstract The time series of groundwater depth has the characteristics of trend, abrupt, and non-stationary. Based on the advantages of wavelet decomposition and long short-term memory neural network (LSTM), a new coupling model(wavelet decomposition-LSTM) for groundwater depth prediction is proposed. Firstly, wavelet decomposition is applied to decompose the groundwater data into high-frequency periodic signals and low-frequency trend signals, to reduce the complexity of the time series. Secondly, the decomposed high-frequency and low-frequency signals are taken as inputs to train the model respectively, and then the total prediction value is acquired. The improved model reduces the limitations of LSTM processing complex signals and improves prediction accuracy. Taking the No. 5 well of Lu Wangfen Town and the No. 3 well of Muye Town as the research object, the achieved results from the proposed model were compared with the results of the LSTM model and the back-propagation (BP) neural network model. This comparison shows that the performance of the new model is better than the others, and the average relative errors of the coupling model are 2.11% and 2.49% respectively. The proposed method has high prediction accuracy and generalization ability and is a more effective method for groundwater depth prediction.

Keywords Groundwater depth, LSTM neural network, Prediction, Wavelet decomposition

Introduction

Groundwater depth is an important indicator reflecting the change of groundwater resources, affected by mining, recharge, evaporation, and other factors, groundwater depth sequence has the characteristics of randomness, uncertainty, and non-stability, which adds a certain degree of difficulty to scientifically and accurately predict groundwater depth(He et al.,2021). When groundwater is overexploited, groundwater funnels and ground subsidence are formed. When the amount of recharge exceeds the amount mined, the groundwater depth becomes shallow. Therefore, predicting the change of groundwater depth is of great importance to regional water resources management and accurate prediction of groundwater depth change can provide a theoretical basis for groundwater protection, planting structure and mode adjustment, rational utilization of water and soil resources, and ecological environmental protection(Alani et al.,2020; Pham et al.,2022; Samantaray et al.,2022; Liu et al.,2022).

The research of groundwater depth prediction models is always one of the hot issues in the water conservancy field at home and abroad. Scholars at home and abroad have done a lot of research on the prediction of groundwater depth and achieved fruitful results. For example, Takafuji et al.(2019) used the time series method of the Auto-Regressive Moving Average Model (ARMA) and the geostatistical method of Symmetric Gauss-Seidel (SGS) to predict the change of groundwater level in the Bauru region of Brazil. Fijani et al.(2013) used fuzzy logic models to simulate the groundwater level in Iran's Maragheh-Bonab region. Shen et al.(2006) used the grey memory model to predict the depth of groundwater in Hotan, Xinjiang. Nadiri et al.(2017) use genetic algorithms to select the number of hidden layers and nodes, optimizing the Deep Neural Network (DNN) model of water level prediction. Aiming at the problem of low accuracy in groundwater depth prediction, Huang et al.(2015) proposed a nonlinear prediction model based on Particle

Swarm Optimization (PSO) Support Vector Machine (SVM). They analyzed the essential characteristics of the development and evolution of the groundwater level system by establishing a PSO-SVM model. From the above, it can be seen that there are many methods for researchers at home and abroad to predict the depth of groundwater, mainly focusing on regression analysis, fuzzy logic, gray theory, neural networks, and genetic algorithms of groundwater time series. The above method has significant advantages in predicting groundwater, but its problems cannot be ignored. In the regression analysis prediction groundwater depth sequence, which factor to use and what expression to use is only a speculation, which in turn affects the unpredictability of some factors, making regression analysis limited in predicting groundwater. When fuzzy logic predicts groundwater, predictors and their weights are difficult to determine and can lead to useful information being ignored. The grey theory predicts the depth of groundwater and obtains a monotonic sequence, and the calculated results are difficult to reflect the change in the time series of the original groundwater depth. Common algorithms such as recurrent neural networks (RNN) have problems with gradient disappearance or gradient explosion. Long short-term memory neural networks (LSTM) have been designed from the beginning to solve long-term dependency problems common in general recurrent neural networks(Liu et al.,2019; Hu et al.,2018; Han et al.,2021). Using LSTM to efficiently transfer and express long-term sequences without causing useful information from long ago to be ignored. At the same time, LSTM can also solve the problem of gradient disappearance/encoding in RNN. LSTM neural networks have strong adaptability and generalization ability of self-learning and are widely used in nonlinear time series prediction. Wavelet decomposition can decompose the groundwater sequence into high-frequency signals and low-frequency signals, the high-frequency component represents the periodic fluctuation water level of the groundwater level, and the low-frequency component represents the trend item water level of the groundwater level, to realize the smoothing treatment of the non-stationary sequence(Tian et al.,2020; Wang et al.,2021; Ghanbarzadeh et al.,2020). By predicting the high-frequency components and low-frequency components separately, the prediction accuracy of non-stationary signals can be effectively improved. Therefore, this paper combines the advantages of wavelet decomposition and the LSTM neural network to establish a groundwater depth prediction coupling model (wavelet decomposition-LSTM) based on the wavelet decomposition LSTM neural network. The use of wavelet decomposition can decompose the information in different frequency bands of the original data, greatly reducing the complexity of the data, combined with the LSTM neural network has a strong advantage in predicting time series data and realizing high-precision prediction of groundwater level.

In this paper, 15 sets of training data and two sets of prediction data are used to decompose the measured data into 7 high-frequency components and 1 low-frequency component by wavelet decomposition, and then 7 high-frequency components and 1 low-frequency component are used as input data of the LSTM model for prediction. The training group data is used as the training, the prediction group data is used as the verification, and the predicted data is added to obtain the prediction value and the measured data to verify the prediction accuracy of the wavelet decomposition-LSTM model. At the same time, the prediction results of the wavelet decomposition-LSTM model are compared with those of a single LSTM neural network and BP neural network to further demonstrate the superiority of the wavelet decomposition-LSTM model.

Materials and methods

Study area

The study included groundwater depth data in Lu Wangfen Town, Xinxiang City, Henan Province, and groundwater depth data in Muye Town. Lu Wangfen Town, has a warm temperate continental monsoon climate, with an annual average temperature of 14 °C, an average temperature of 0.1 °C in January, an average temperature of 27.2 °C in July, average annual precipitation of 586.32 mm, annual evaporation of 1748.4 mm, and rainfall concentrated in June to September every year. Muye Town has a warm temperate continental monsoon climate with four distinct seasons and an average annual precipitation of 600.5 mm. Through the comprehensive and scientific monitoring of the groundwater in Lu Wangfen Town and Muye Town, the dynamic characteristics of groundwater, the understanding of the Spatiotemporal evolution of groundwater, and the grasp of its dynamic change characteristics. On this basis, the groundwater depth is predicted, and the variation trend of groundwater level is analyzed, to provide a theoretical basis for the sustainable utilization of groundwater resources, the ecological environment security, and the sustainable and healthy development of the social economy. The data in this paper are derived from the monitoring data of the No. 5 Professional Observation Well in Lu Wangfen Town and No. 3 Professional Observation Well in Muye Town, Xinxiang City from 2005 to 2021, which can fully reflect the real dynamic changes of groundwater, and the monitoring data is well represented, meeting the technical requirements of groundwater monitoring specifications. The location of the two wells is shown in Fig.1. The yearly variation curve of groundwater depth is shown in Fig. 2 and Fig. 3.

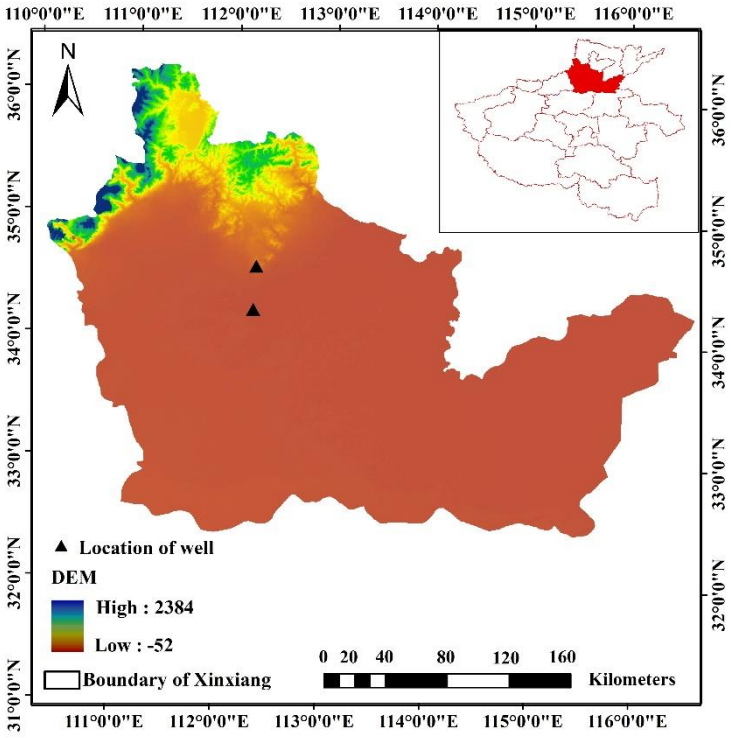

Fig.1 Location map of the two wells

Fig.2 Groundwater depth curve of Well No. 5 in Lu Wangfen Town, Xinxiang City from 2005 to 2021

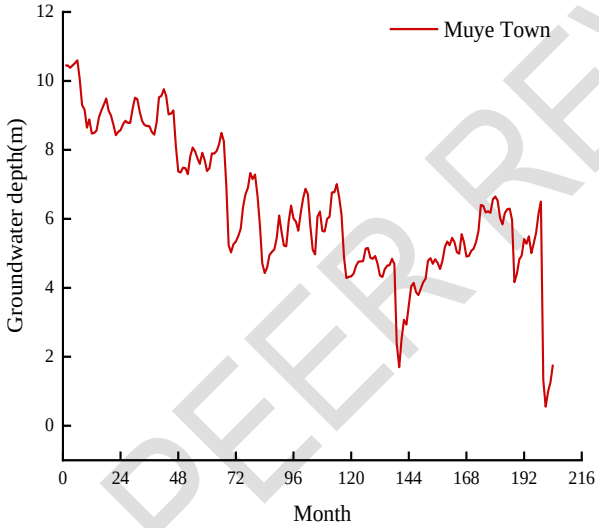

Fig.3 Groundwater depth curve of Well No. 3 in Muye Town, Xinxiang City from 2005 to 2021

Wavelet transform

Fourier transform is a widely used analytical method in signal processing, which can convert time-domain signals into frequency-domain signals, but Fourier transform has no discrimination ability in the time domain(Nanda et al.,2016; Sehgal et al.,2014; Zhang et al.,2018). The wavelet transform is developed given the shortcomings of the Fourier transform, and the original time-domain functions are decomposed by using wavelets and family band-pass filters, and the signal is decomposed into two-dimensional time-frequency information, which greatly enhances the performance ability of local signals and improves the noise immunity of the model. The wavelet transform is a data decomposition and reconstruction method, which first uses a low-pass filter and a high-pass filter to decompose the original data into low-frequency wavelet coefficient cA_n and high-frequency wavelet coefficient $cD_1,\cdots,cD_n$, respectively. The low-frequency wavelet coefficient can be further decomposed, and the process can be iterated several times until the maximum number of decompositions is reached. $\psi(t)$ wavelet transform can be divided into continuous wavelet transform (CWT) and discrete wavelet transform (DWT). In order to improve the ability of continuous wavelet

transforms to deal with complex problems, CWT transforms the fundamental wavelets as follows:

$$\psi_{ab}(t) = a^{-\frac{1}{2}}\psi\left(\frac{t-b}{a}\right) \tag{1}$$

Where, a is the scaling factor $(a>0)$ and b is the translation factor $(b \in R)$. By adjusting the values of a and b to control the scale of the wavelet transform, the time subdivision at high frequency and frequency subdivision at low frequency can be achieved, and the requirements of adaptive time-frequency signal analysis can be realized.

The formula for the continuous wavelet transform is as follows:

$$Wf(a,b) = \int_{-\infty}^{+\infty} f(t)\overline{\psi_{ab}(t)}\mathrm{d}t \tag{2}$$

Where, $W_f(a,b)$ represents the continuous wavelet coefficient. $f(t)$ represents the raw data. $\overline{\psi_{ab}(t)}$ represents the conjugate function of $\psi_{ab}(t)$. However, continuous wavelet transforms calculate wavelet coefficients on all scales, and this time-consuming process also produces a lot of redundant data. Therefore, discrete wavelet transforms are usually used in practical processes. The discrete wavelet transform is obtained by discretizing the continuous wavelet transform at scales and displacements at a power of 2. The calculation method of a and b in the $\psi_{ab}(t)$ function is shown in Equation (3):

$$a = a_0^{\,j}, b = ka_0^{\,j}b_0 \tag{3}$$

Where, $a_0 > 0, b_0 \in R, \forall j,k = 0,1,2,\cdots, m \in Z$. Then the calculation method of function $\psi_{jk}(t)$ is shown in Equation (4):

$$\psi_{jk}(t) = a_0^{-\frac{j}{2}}\psi\left(a_0^{-j}t - kb_0\right) \tag{4}$$

The formula for the discrete wavelet transform is as follows:

$$Wf(j,k) = \int_{-\infty}^{+\infty} f(t)\overline{\psi_{jk}(t)}\mathrm{d}t \tag{5}$$

Where, $Wf(j,k)$ represents the discrete wavelet coefficient. $f(t)$ represents the raw data. $\overline{\psi_{jk}(t)}$ represents the conjugate function of $\psi_{jk}(t)$.

LSTM neural network

LSTM is a special type of RNN that effectively avoids the problem of gradient diffusion of RNN in long-dependent sequence models. The LSTM model includes four parts: input gate, forgetting gate, output gate, and cell state. The input gate determines how much input information is passed to the cell state. The forgetting gate mainly controls how much

information in the cell state in the previous period is forgotten and how much is transmitted to the current moment. The output gate is based on the cell state of the forgetting gate and the input gate outputs the calculation results. The cell state is used to record information in the current input, the state of the hidden layer at the previous moment, the state of the cell at the previous moment, and the gate structure. Fig. 4 shows the internal structure of the LSTM hidden layer, where f_t, i_t, and o_t represent the values of the t moment forgetting gate, the input gate, and the output gate, respectively, and a_t represents the preliminary feature extraction of $h(t-1)$ and x_t at the t time.

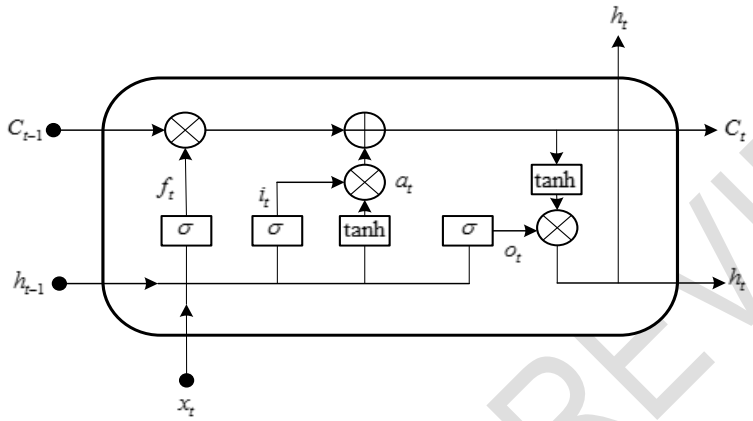

Fig.4 LSTM neural network internal structure diagram

$$f(t)=\sigma\left(Wfh_{t-1}+Ufx_t+b_f\right) \tag{6}$$

$$i(t)=\sigma\left(W_ih_{t-1}+U_ix_t+b_i\right) \tag{7}$$

$$a(t)=\tanh\left(W_ah_{t-1}+U_ax_t+b_a\right) \tag{8}$$

$$o(t)=\sigma\left(W_oh_{t-1}+U_ox_t+b_o\right) \tag{9}$$

Where, x_t represents the input at moment t. h_{t-1} represents the hidden state value at moment $t-1$. W_f, W_i, W_o and W_a represent the weight coefficients of the forgetting gate, the input gate, the output gate, and h_{t-1} during feature extraction, respectively. U_f, U_i, U_o and U_a represent the weight coefficients of x_t during the forgetting gate, input gate, output gate, and feature extraction, respectively. b_f, b_i, b_o and b_a represent the forgetting gate, input gate, output gate, and bias values during feature extraction, respectively. $\tanh$ represents the tangent hyperbolic function and σ represents the activation function.

$$\tanh(x)=\frac{1-e^{-2x}}{1+e^{-2x}} \tag{10}$$

$$\sigma(x)=\frac{1}{1+e^{-x}} \tag{11}$$

The results of the forgetting gate and input gate calculations act on $c(t-1)$, constituting the cell state $c(t)$ at the t moment.

$$c(t) = c(t-1) \square f(t) + i(t) \square a(t) \quad (12)$$

Where, $\square$ is the Hadamard product.

Finally, the hidden layer state $h(t)$ at moment t is solved by the output gate $o(t)$ and the cell state $c(t)$ at the current moment.

$$h(t) = o(t) \square \tanh(c(t)) \quad (13)$$

Data analysis

Based on the wavelet decomposition principle, the contribution of each frequency domain component after decomposition to the original sequence is different. For the groundwater depth sequence, the component with a large contribution rate determines the change of the sequence to a certain extent, which can be understood as the driving factor of its change. Thus, predictions of groundwater depths can be broken down into predictions of their composition. The calculation steps for wavelet decomposition and the LSTM network prediction model are as follows:

1. The original sequence of groundwater depth is divided into high-frequency components and low-frequency components by wavelet decomposition.

2. The high and low-frequency components of groundwater depth in 2005-2019 are used as the training data of the LSTM network, and the high and low-frequency components of 2020-2021 are used as the prediction data of the LSTM network.

3. Use the LSTM neural network to predict the high and low-frequency components of groundwater depth in 2020-2021.

4. The predicted high and low-frequency components of groundwater depth are added to obtain the predicted value, and then the predicted value is subtracted from the true value to obtain the absolute error, and the absolute error is divided by the real value to obtain the relative error.

The specific process is shown in Fig. 5.

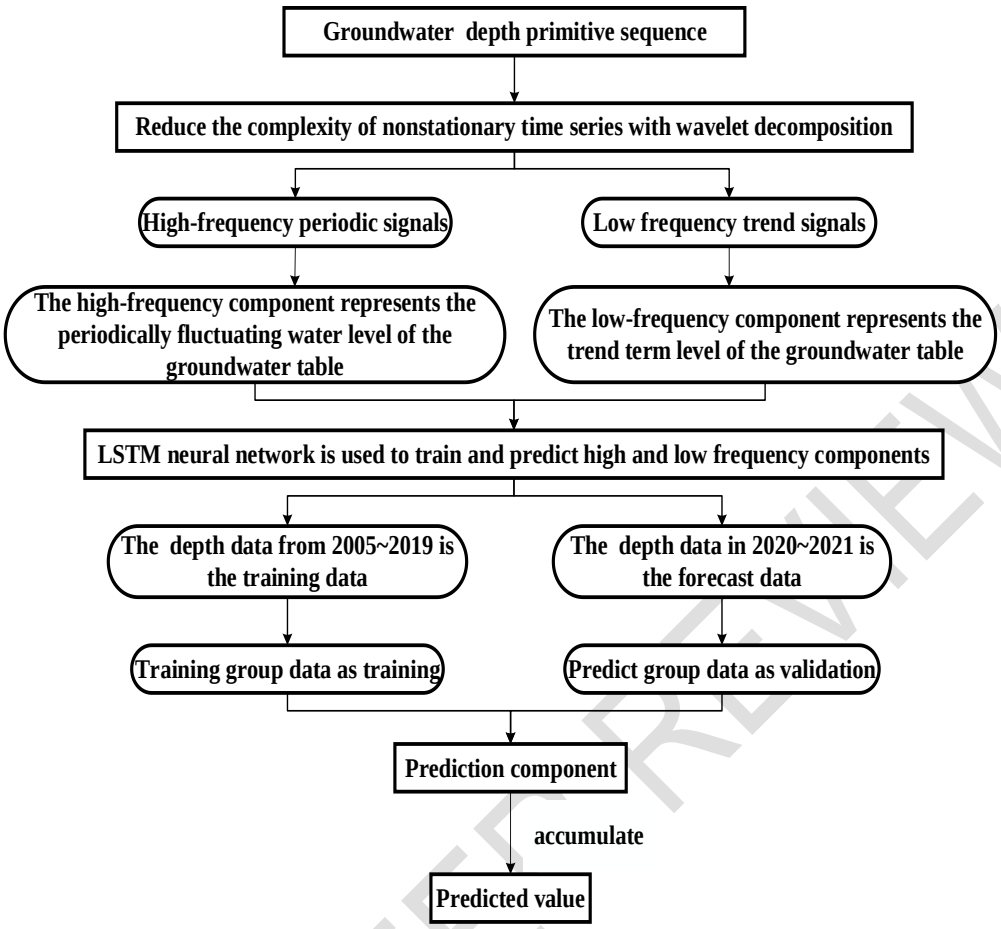

Fig. 5 Wavelet decomposition-LSTM model prediction flowchart

Results and discussion

As can be seen from Figure 2 and Figure 3, from 2005 to 2021, the groundwater depth of Lu Wangfen Town and Muye Town showed a general downward trend, accompanied by certain fluctuations in the decline process, and the fluctuation amplitude was inconsistent, which also verified that the groundwater depth was uncertain and non-stable, which also reflected the rationality of the method of using wavelet decomposition from the side.

Wavelet decomposition

According to the steps of wavelet decomposition earlier, wavelet decomposition of groundwater depth data from 2005 to 2021 in Lu Wangfen Town was performed. The decomposition results are shown in Fig. 6.

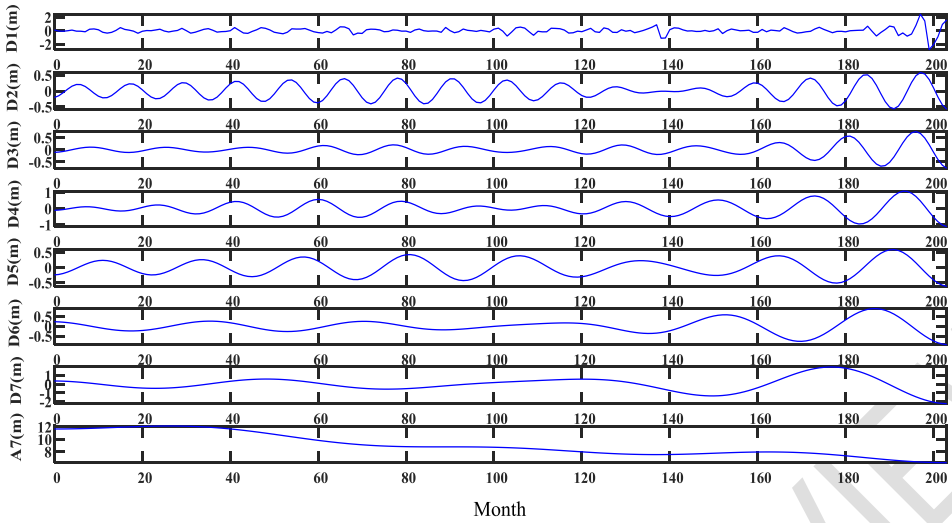

Fig.6 Wavelet decomposition diagram of groundwater depth in Lu Wangfen Town, 2005-2021

As can be seen from Fig. 6, the groundwater depth sequence is decomposed into 7 high-frequency components D1, D2, D3, D4, D5, D6, D7, and a low-frequency component A7. From D1 to D7, the frequency of each component gradually decreases, the wavelength becomes shorter, the volatility decreases, and the values of the seven high-frequency components are small, while the values of the low-frequency components are larger. Xinxiang City Lu Wangfen Town No. 5 professional observation well groundwater depth sequence, after wavelet decomposition, the volatility and non-stationarity of the sequence are greatly reduced.

Groundwater depth prediction

From the perspective of wavelet decomposition, the contribution rate of each high and low-frequency component to the groundwater depth sequence is not the same, and it can be approximated that the high and low-frequency components are regarded as the driving factors of groundwater depth, and the groundwater depth prediction is equivalent to the prediction of high and low-frequency components.

When using the LSTM network to predict the groundwater depth of the No. 5 professional observation well in Lu Wangfen Town, Xinxiang City, it is necessary to divide the training samples and test samples. The D1 to D7 component data from 2005 to 2019 were used as training samples, and the D1 to D7 components and A7 component data from 2020 to 2021 were used as test samples.

Through a large number of experiments, it is best to find that LSTM has 200 hidden units. To prevent the gradient from exploding, set the gradient threshold to 1, specify an initial learning rate of 0.005, and reduce the learning rate by a multiplicative coefficient of 0.2 after 125 rounds of training.

According to the previous steps, the D1 to D7 components and A7 components in the groundwater depth of Lu Wangfen Town No. 5 in Xinxiang City were predicted by using the LSTM network. The prediction results are shown in Fig. 7, and the error analysis results are shown in Table 1.

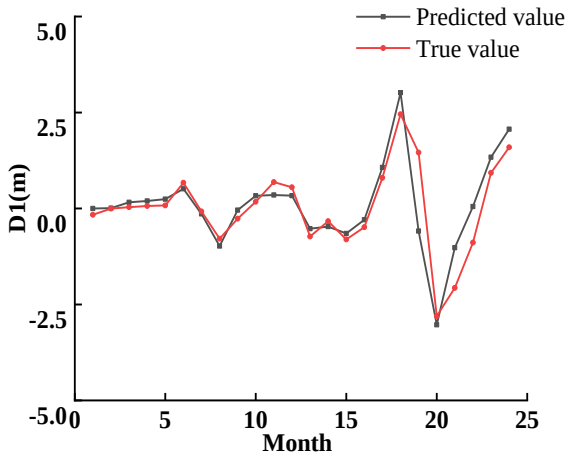

(a) D1

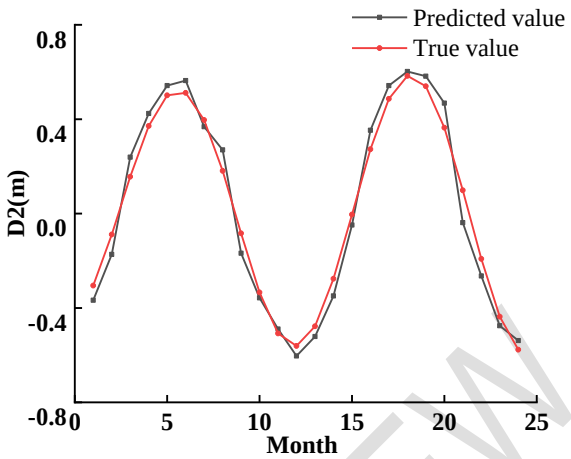

(b) D2

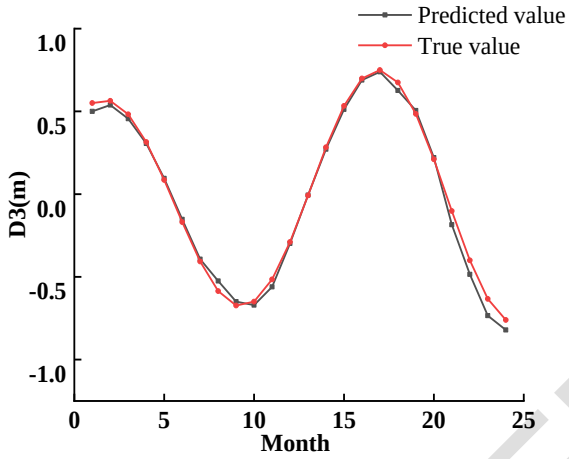

(c) D3

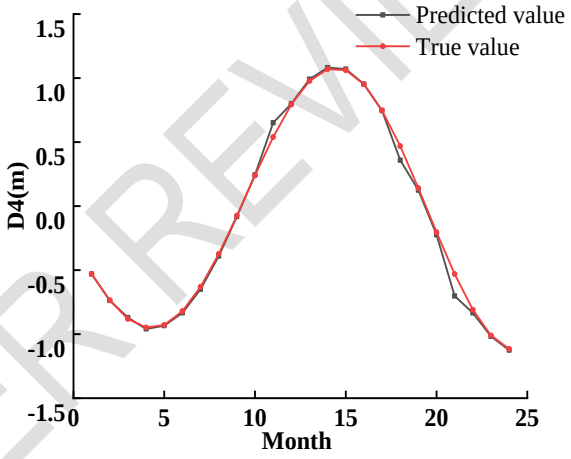

(d) D4

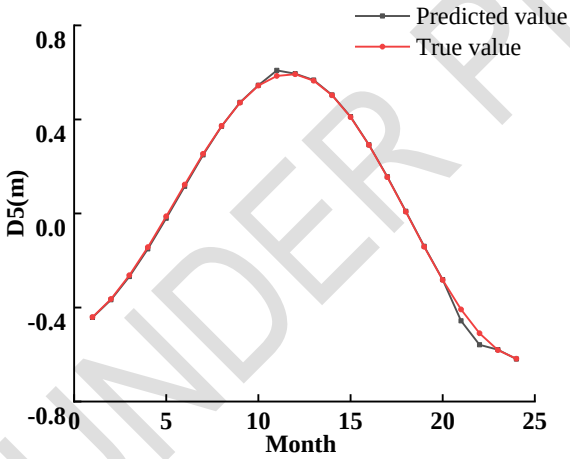

(e) D5

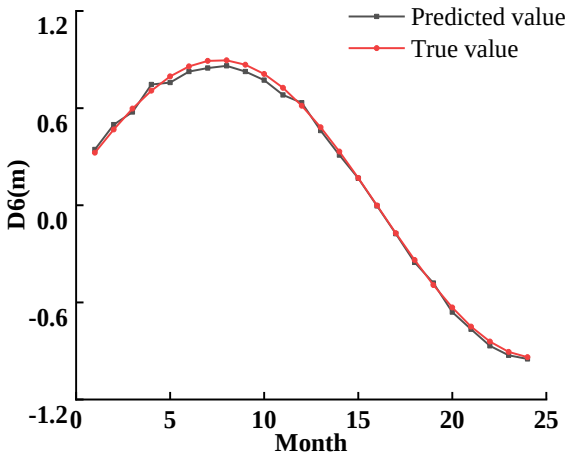

(f) D6

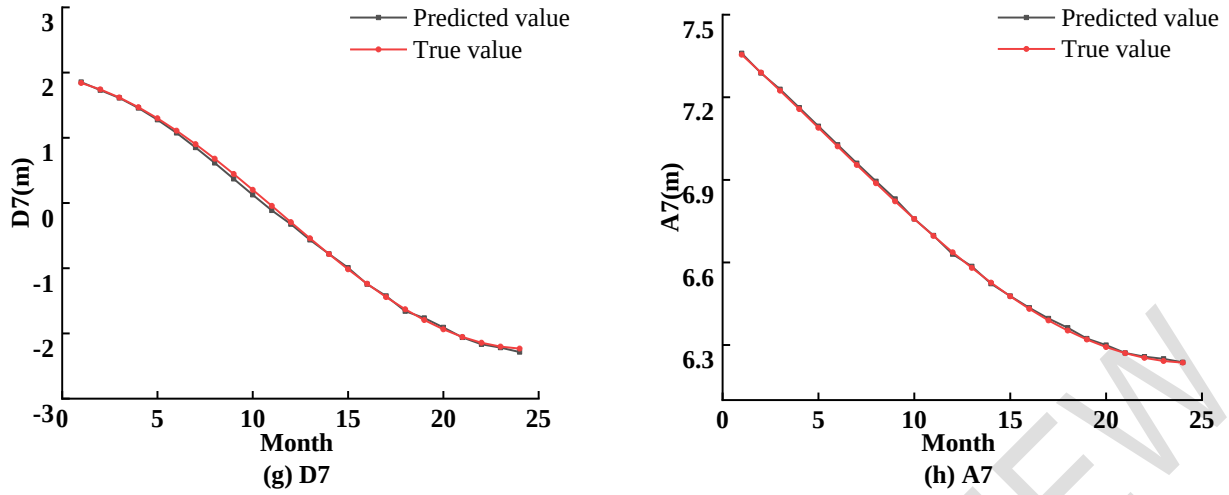

Fig.7 Prediction results of D1~D7 and A7 in Lu Wangfen Town

Table 1 The relative error index of D1 ~ A7

Prediction object	Maximum relative error(%)	Minimum relative error(%)	Average relative error(%)
D1	461.35	19.49	107.22
D2	248.30	1.33	37.72
D3	186.64	1.26	26.23
D4	153.95	0.30	18.96
D5	139.04	0.25	13.15
D6	73.11	0.22	9.28
D7	69.94	0.12	7.02
A7	0.59	0.01	0.21

As can be seen from Table 1: the maximum relative errors of high-frequency components D1 to D7 are relatively large, which are 461.35%, 248.30%, 186.64%, 153.95%, 139.04%, 73.11%, 69.94%, and 0.59%, respectively. The minimum relative error and average relative error of D1 are also very large, which are 19.49% and 107.22% respectively. The minimum relative errors of D2 to A7 are very small, which are 1.33%, 1.26%, 0.30%, 0.25%, 022%, 0.12%, and 0.01%, respectively. The average relative errors of D2 and D3 are also relatively large, which are 37.72% and 26.23%, respectively. The low-frequency component A7 has the best prediction effect, and the maximum relative error, minimum relative error, and average relative error are 0.59%, 0.01%, and 0.21%, respectively. As can be seen from Table 1, after the wavelet decomposition of the groundwater depth series, the high-frequency components become more stable, and the average relative errors from D1 to A7 show a downward trend on the whole. Although some points in D1 to D7 have large errors, the proportion of individual points in the groundwater depth series is small and will not affect the overall error of groundwater depth.

To visually see the prediction effect of the model, the predicted value of groundwater depth obtained month by month from 2020 to 2021 is compared with the real value (Fig. 8), and the prediction error is shown in Table 2.

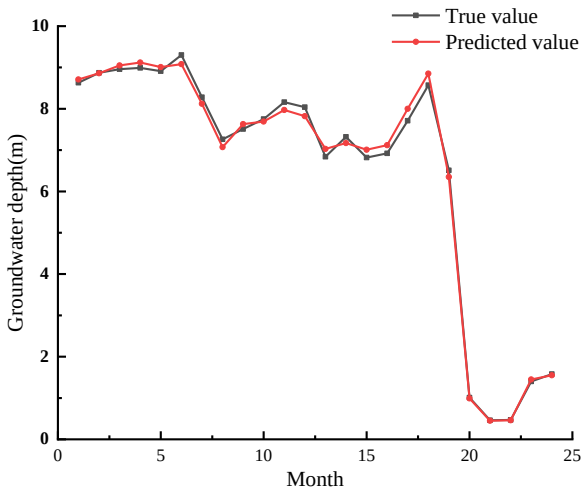

Fig.8 Prediction curve of groundwater depth in Lu Wangfen Town from 2020 to 2021

Table 2 Groundwater depth prediction error in Lu Wangfen Town from 2020 to 2021

Year	Month	True value(m)	Predicted value(m)	Absolute error(m)	Relative error (%)
2020	1	8.63	8.71	0.08	0.93
	2	8.87	8.86	-0.01	0.11
	3	8.96	9.05	0.09	1.00
	4	8.99	9.12	0.13	1.45
	5	8.91	9.01	0.10	1.12
	6	9.30	9.08	-0.22	2.37
	7	8.28	8.12	-0.16	1.93
	8	7.26	7.07	-0.19	2.62
	9	7.51	7.63	0.12	1.60
	10	7.75	7.69	-0.06	0.77
	11	8.16	7.97	-0.19	2.33
	12	8.04	7.82	-0.22	2.74
2021	1	6.84	7.03	0.19	2.78
	2	7.32	7.17	-0.15	2.05
	3	6.82	7.01	0.19	2.79
	4	6.92	7.12	0.20	2.89
	5	7.71	8.00	0.29	3.76
	6	8.57	8.85	0.28	3.27
	7	6.51	6.35	-0.16	2.46
	8	1.01	0.99	-0.02	1.98
	9	0.46	0.45	-0.01	2.17
	10	0.47	0.46	0.01	2.13
	11	1.40	1.45	0.05	3.57
	12	1.59	1.55	-0.03	1.90
The average relative error(%)				2.11	

In order to compare and verify the accuracy of the models, separate LSTM neural network model and back-propagation (BP) neural network model were used to predict the monthly groundwater depth sequence of the No. 5 well in Lu Wangfen Town from 2020 to 2021, and the prediction error was shown in Table 3, and the comparison was shown in Fig. 9.

Table 3 Comparison of wavelet decomposition-LSTM model in Lu Wangfen Town with other models

Year	Month	Wavelet decomposition-LSTM model relative error(%)	LSTM model relative error(%)	BP model relative error(%)
2020	1	0.93	2.79	3.54
	2	0.11	0.66	2.59
	3	1.00	3.69	3.83
	4	1.45	0.69	14.28
	5	1.12	2.70	6.78
	6	2.37	3.34	4.32
	7	1.93	11.91	7.85
	8	2.62	8.78	5.43
	9	1.60	4.63	3.21
	10	0.77	10.98	2.58
	11	2.33	6.56	8.33
	12	2.74	9.87	3.85
2021	1	2.78	18.89	6.68
	2	2.05	1.24	5.34
	3	2.79	3.61	3.29
	4	2.89	6.67	1.58
	5	3.76	9.58	2.27
	6	3.27	1.85	4.33
	7	2.46	1.58	6.53
	8	1.98	14.31	5.43
	9	2.17	13.62	8.86
	10	2.13	17.98	7.54
	11	3.57	15.28	3.32
	12	1.90	10.6	5.89

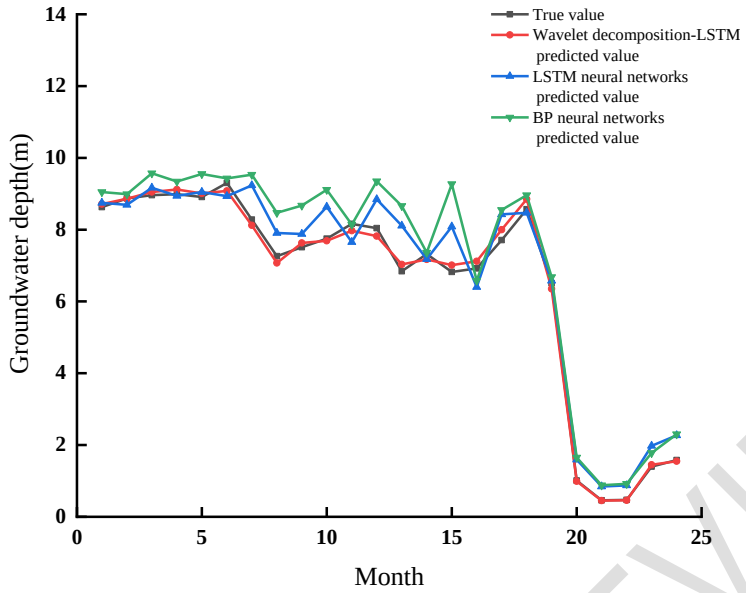

Fig.9 Comparison of the prediction results of the Lu Wangfen Town wavelet decomposition-LSTM model with other models

The specific prediction steps of Muye Town are the same as Lu Wangfen Town, and the prediction error of the groundwater depth prediction is shown in Table 4, and the separate LSTM neural network model and the BP neural network model are used to predict the monthly groundwater depth sequence of Muye Town No. 3 well from 2020 to 2021, and the prediction error is shown in Table 5. The comparison is shown in Fig. 10.

Table 4 Groundwater depth prediction error in Muye Town from 2020 to 2021

Year	Month	True value(m)	Predicted value(m)	Absolute error(m)	Relative error (%)
2020	1	6.63	6.51	-0.12	1.81
	2	6.11	6.06	-0.05	0.82
	3	5.91	5.92	0.01	0.17
	4	6.22	6.21	-0.01	0.16
	5	6.31	6.49	0.18	2.85
	6	6.30	6.41	0.11	1.75
	7	5.96	5.73	-0.23	3.86
	8	4.15	4.29	0.14	3.37
	9	4.38	4.22	-0.16	3.65
	10	4.79	4.68	-0.11	2.30
	11	4.92	5.03	0.11	2.24
	12	5.42	5.34	-0.08	1.48
2021	1	5.32	5.21	-0.11	2.07
	2	5.54	5.33	-0.21	3.79
	3	5.07	4.89	-0.18	3.55
	4	5.34	5.15	-0.19	3.56

	5	5.62	5.84	0.22	3.91
	6	6.17	6.28	0.11	1.78
	7	6.48	6.26	-0.22	3.40
	8	1.28	1.23	-0.05	3.91
	9	0.51	0.49	-0.02	3.92
	10	0.95	0.97	0.02	2.11
	11	1.22	1.24	0.02	1.64
	12	1.72	1.75	0.03	1.74
The average relative error(%)				2.49	

Table 5 Comparison of wavelet decomposition-LSTM model in Muye Town with other models

Year	Month	Wavelet decomposition-LSTM model relative error(%)	LSTM model relative error(%)	BP model relative error(%)
2020	1	1.81	3.42	3.14
	2	0.82	7.14	5.08
	3	0.17	0.34	7.73
	4	0.16	0.17	11.15
	5	2.85	9.07	5.38
	6	1.75	12.99	6.82
	7	3.86	2.90	4.66
	8	3.37	17.06	7.87
	9	3.65	14.19	10.25
	10	2.30	2.43	6.27
	11	2.24	15.38	3.58
	12	1.48	3.68	4.77
2021	1	2.07	1.46	6.73
	2	3.79	5.64	1.65
	3	3.55	17.94	2.87
	4	3.56	1.22	10.45
	5	3.91	4.14	3.58
	6	1.78	8.86	4.21
	7	3.40	9.23	6.44
	8	3.91	13.04	2.89
	9	3.92	19.57	1.08
	10	2.11	10.73	7.85
	11	1.64	14.56	5.21
	12	1.74	12.48	4.33

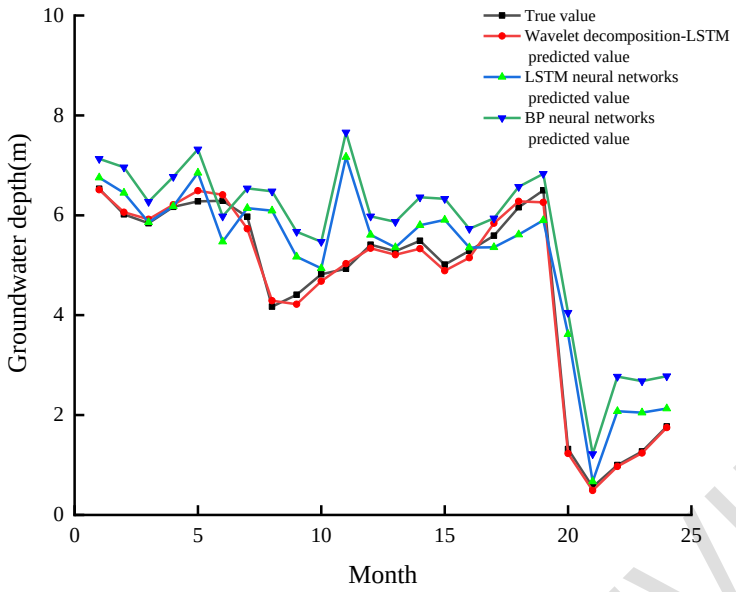

Fig.10 Comparison of the prediction results of the Muye Town wavelet decomposition-LSTM model with other models

By comparing the results with the results of the LSTM neural network model and the BP neural network model alone, it can be seen that the average relative error predicted by the LSTM neural network model alone in Lu Wangfen Town and Muye Town is 7.58% and 8.65%. The average relative error of the prediction of the BP neural network model was 5.32% and 5.58%, while the average relative error of the wavelet decomposition-LSTM neural network model was 2.11% and 2.49%, indicating that the wavelet decomposition-LSTM neural network model predicted the groundwater depth with good effect.

Conclusions

In this paper, wavelet decomposition is combined with the LSTM neural network model, the wavelet decomposition-LSTM neural network model is established, and it is applied to the groundwater depth prediction of No. 5 well in Lu Wangfen Town and No. 3 well in Muye Town, to verify the reliability of the model, the results are compared with the results of separate LSTM neural network model and BP neural network model, and the following conclusions are drawn:

1. The groundwater depth time series is decomposed by wavelets, and the signal is decomposed into several high-frequency components and low-frequency components, and the predicted value is equal to the predicted value of several high-frequency components and low-frequency components. Although some high-frequency components have relatively large prediction errors, these high-frequency components account for less of the entire signal, and the overall error will be reduced when the predicted values of the high-frequency components and low-frequency components are converted into overall predictions.

2. The groundwater results predicted by the separate LSTM neural network model and the BP neural network model were compared with the prediction results of the wavelet decomposition-LSTM neural network model, and the average relative error predicted by the LSTM neural network model alone was 7.58% and 8.65%, the average relative error predicted by the BP neural network model was 5.32% and 5.58%, and the average relative error predicted by the wavelet decomposition-LSTM neural network model was 2.11% and 2.49%. It shows that the wavelet decomposition-LSTM

neural network model can better predict groundwater depth.

3. The wavelet decomposition-LSTM coupling model proposed in this paper predicts LSTM after the original information is processed by wavelet decomposition, which reduces the non-stationarity of the original groundwater buried depth time series, enhances the prediction accuracy of LSTM for nonstationary signals, and predicts the distribution of groundwater more scientifically and accurately. This method provides another technical means for the research of shallow groundwater exploration, which is of practical significance to engineering practice.

References

Alani, R., Nwude, D., Joseph, A., & Akinrinade, O. (2020). Impact of gas flaring on surface and underground water: a case study of Anieze and Okwuibome areas of Delta State, Nigeria. *Environmental monitoring and assessment*, 192(3), 1-10.

Pham Q B, Kumar M, Di Nunno F, et al. Groundwater level prediction using machine learning algorithms in a drought-prone area[J]. Neural Computing and Applications, 2022, 34(13): 10751-10773.

Samantaray S, Biswakalyani C, Singh D K, et al. Prediction of groundwater fluctuation based on hybrid ANFIS-GWO approach in arid Watershed, India[J]. Soft Computing, 2022, 26(11): 5251-5273.

Liu Q, Gui D, Zhang L, et al. Simulation of regional groundwater levels in arid regions using interpretable machine learning models[J]. Science of The Total Environment, 2022, 831: 154902.

Fijani, E., Nadiri, A. A., Moghaddam, A. A., Tsai, F. T. C., & Dixon, B. (2013). Optimization of drastic method by supervised committee machine artificial intelligence to assess groundwater vulnerability for maragheh–bonab plain aquifer, Iran. *Journal of hydrology*, 503, 89-100.

Ghanbarzadeh, M., & Aminghafari, M.(2020). A novel wavelet artificial neural networks method to predict non-stationary time series. *Communications in statistics-theory and methods*, 49(4), 864-878.

He, L., Hou, M., Chen, S., Zhang, J., Chen, J., & Qi, H. (2021). Construction of a spatio-temporal coupling model for groundwater level prediction: A case study of Changwu area, Yangtze River Delta region of China. *Water Supply*, 21(7), 3790-3809.

Huang, F. M., Yin, K. L., Zhang, G. R., Tang, Z. Z., & Zhang, J. (2015). Prediction of groundwater level in landslide using multivariable PSO-SVM model. *Journal of Zhejiang University (Engineering Science)*, 49(6), 1193-1200.

Hu, C., Wu, Q., Li, H., Jian, S., Li, N., & Lou, Z. (2018). Deep learning with a long short-term memory networks approach for rainfall-runoff simulation. *Water*, 10(11), 1543.

Han, H., Choi, C., Jung, J., & Kim, H. S. (2021). Deep learning with long short term memory based Sequence-to-Sequence model for Rainfall-Runoff simulation. *Water*, 13(4), 437.

Liu, P., Wang, J., Sangaiah, A. K., Xie, Y., & Yin, X. (2019). Analysis and prediction of water quality using LSTM deep neural networks in IoT environment. *Sustainability*, 11(7), 2058.

Nadiri, A. A., Gharekhani, M., Khatibi, R., & Moghaddam, A. A. (2017). Assessment of groundwater vulnerability using supervised committee to combine fuzzy logic models. *Environmental Science and Pollution Research*, 24(9),

8562-8577.

Nanda, T., Sahoo, B., Beria, H., & Chatterjee, C. (2016). A wavelet-based non-linear autoregressive with exogenous inputs (WNARX) dynamic neural network model for real-time flood forecasting using satellite-based rainfall products. *Journal of Hydrology*,539, 57-73.

Shen, B., Liu, M. & Huang, L. M. (2006). Grey self-memory model and its application in the prediction of groundwater depth in Hotan, Xinjiang. *Journal of Northwest A & F University* (*Natural Science Edition*), 34(11), 223-226.

Sehgal, V., Tiwari, M. K., & Chatterjee, C. (2014). Wavelet bootstrap multiple linear regression based hybrid modeling for daily river discharge forecasting. *Water resources management*, 28(10), 2793-2811.

Takafuji, E. H. D. M., Rocha, M. M. D., & Manzione, R. L. (2019). Groundwater level prediction/forecasting and assessment of uncertainty using SGS and ARIMA models: A a case study in the Bauru Aquifer System (Brazil). *Natural Resources Research*, 28(2), 487-503.

Tian, Z. (2020). A combined prediction approach based on wavelet transform for crop water requirement. *Water Supply*, 20(3), 1016-1034.

Wang, H., Lu, H., Alelaumi, S. M., & Yoon, S. W. (2021). A wavelet-based multi-dimensional temporal recurrent neural network for stencil printing performance prediction. *Robotics and Computer-Integrated Manufacturing*,71, 102129.

Zhang, J., Qiu, H., Li, X., Niu, J., Nevers, M. B., Hu, X., & Phanikumar, M. S. (2018). Real-time nowcasting of microbiological water quality at recreational beaches: A wavelet and artificial neural network-based hybrid modeling approach. *Environmental science & technology*, 52(15), 8446-8455.